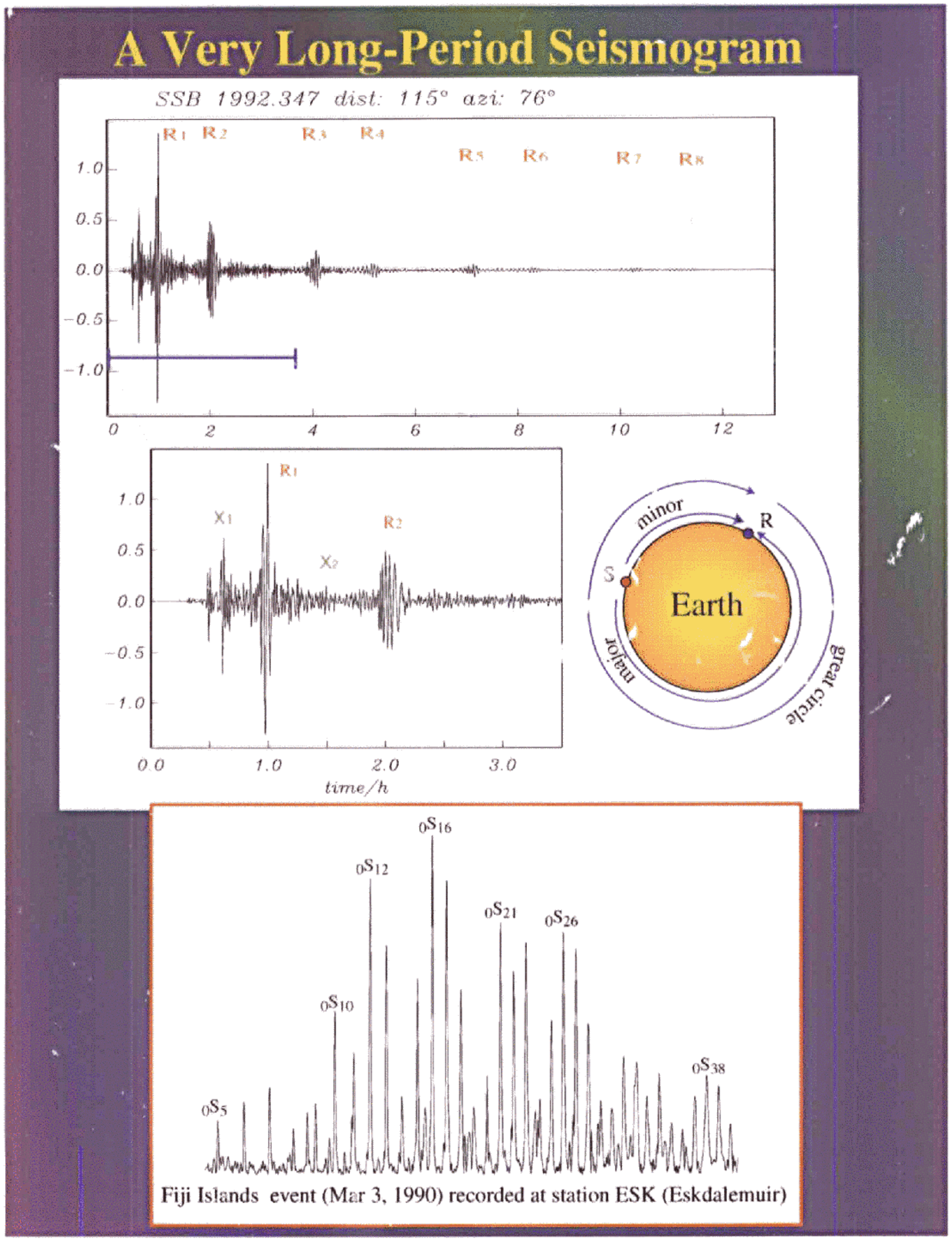

A Very Long-Period Seismogram

Fiji Islands event (Mar 3, 1990) recorded at station ESK (Eskdalemuir)

Modes

$$u(t) = \sum_k A_k \cos(\omega_k t + \phi_k)\, e^{-\alpha_k t}$$

$A_k, \phi_k \Rightarrow$ source

$\omega_k, \alpha_k \Rightarrow$ structure

$\alpha_k = \frac{\omega_k}{2Q_k} \Leftarrow$ "quality"

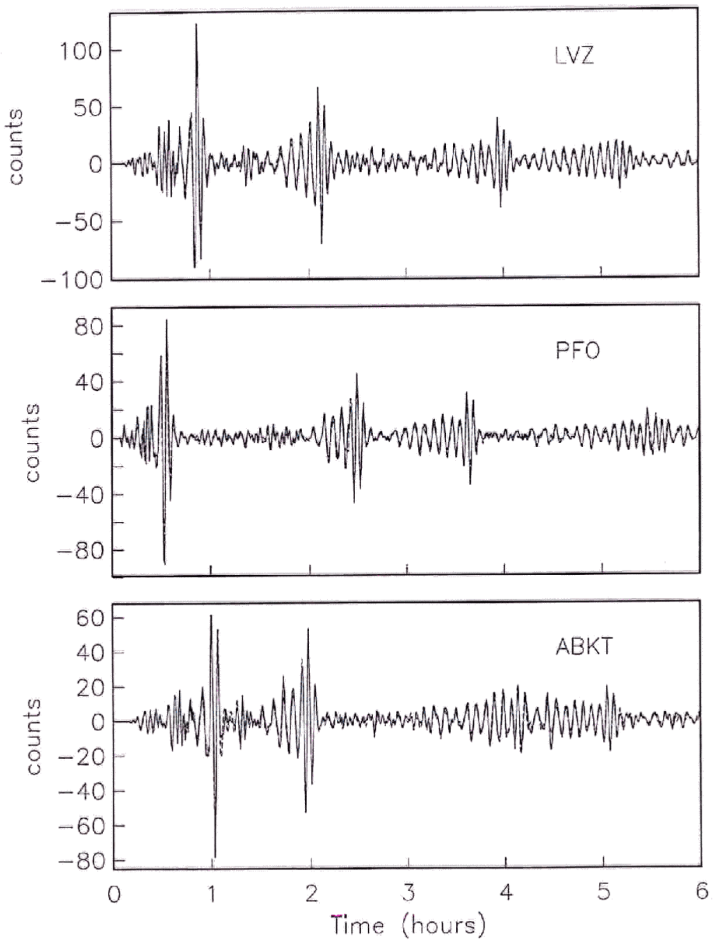

$$C_k(\omega) = \int_0^\infty \cos(\omega_k t) e^{-\alpha_k t} e^{-i\omega t} dt,$$

$$= \tfrac{1}{2} \int_0^\infty (e^{(-\alpha_k + i(\omega_k - \omega))t} + e^{(-\alpha_k - i(\omega_k + \omega))t}) dt,$$

$$= \tfrac{1}{2} \frac{1}{\alpha_k - i(\omega_k - \omega)} + \tfrac{1}{2} \frac{1}{\alpha_k + i(\omega_k + \omega)}.$$

For $\omega \simeq \omega_k$, the first term is large whilst the second term is much smaller. Thus, if we only consider positive frequencies in the vicinity of ω_k, we have

$$C_k(\omega) \simeq \tfrac{1}{2} \frac{1}{\alpha_k - i(\omega_k - \omega)} \tag{1.4}$$

or, in terms of real and imaginary parts,

$$C_k(\omega) = \tfrac{1}{2} \frac{\alpha_k}{\alpha_k^2 + (\omega_k - \omega)^2} + i\tfrac{1}{2} \frac{(\omega_k - \omega)}{\alpha_k^2 + (\omega_k - \omega)^2} \tag{1.5}$$

$C_k(\omega)$ is plotted in Fig. 1.2. Note that the real part falls off from its peak value as $(\omega_k - \omega)^2$ whereas the imaginary part falls off only as $(\omega_k - \omega)$. This latter property means that the spectrum of a decaying sinusoid falls off quite slowly from its peak value ($\approx 6db/octave$).

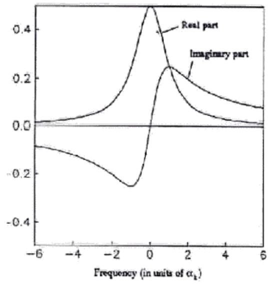

Fig 1.2 Spectrum of a decaying cosinusoid in a small frequency band surrounding the center frequency, ω_k. Frequency is in units of α_k

Problem 1.1 Show that the width of the power spectrum of $C_k(\omega)$ at the half power points is $2\alpha_k$.

The seismogram is a sum of such spectra all centered at different frequencies so a plot of the modulus

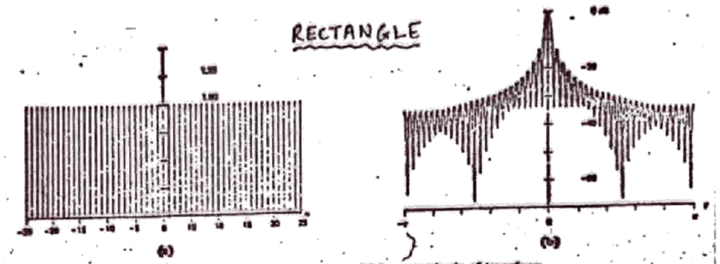

Fig. 15. (a) Rectangle window. (b) Log-magnitude of transform.

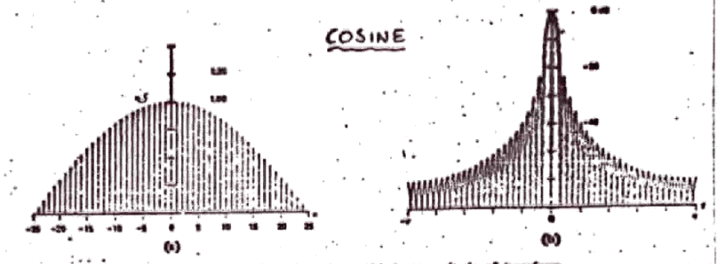

Fig. 16. (a) Cos (πn/N) window. (b) Log-magnitude of transform.

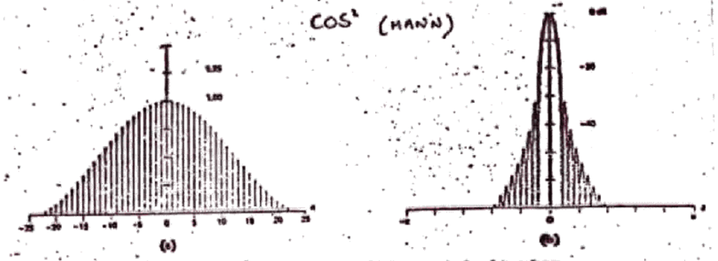

Fig. 17. (a) Cos² (πn/N) window. (b) Log-magnitude of transform.

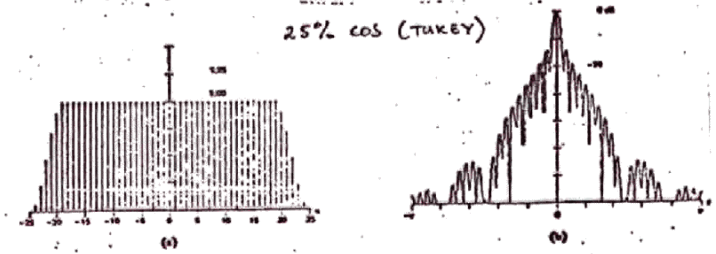

Fig. 30. (a) 25-percent cosine taper (Tukey) window. (b) Log-magnitude of transform.

Figure 1.5. Various tapers and their log amplitude spectra.

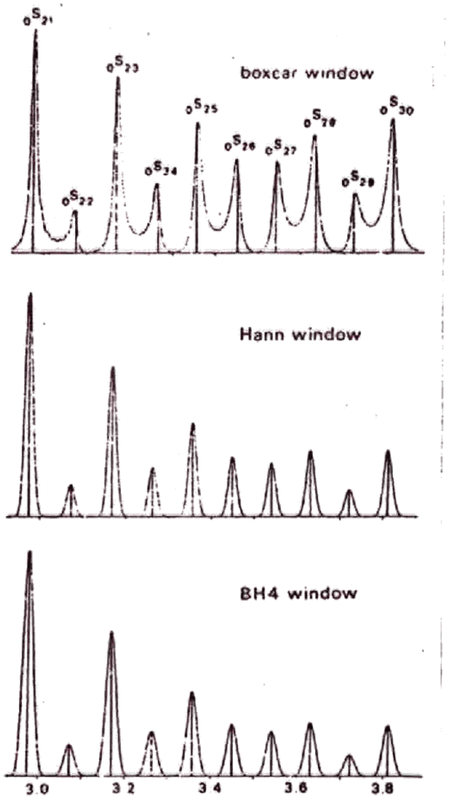

Figure 1.7. The effect of tapering on the spectra of synthetic seismograms which include fundamental modes only. In the top panel, note how peaks appear to be shifted away from their true frequencies

be.

An overview of measurement techniques can be found in Masters and Gilbert, (1983) and we briefly describe two of these here. For simplicity, we consider a single isolated mode of oscillation though it is desirable that any measurement technique can handle modes which overlap in frequency. We have

$$u(t) = A_k \cos(\omega_k t + \phi_k) e^{-\alpha_k t}$$

Fourier transforming gives

$$\rho_0 \frac{\partial^2 \underline{s}}{\partial t^2} = \overset{①}{\nabla\cdot\underline{\underline{T}}} - \overset{②}{\nabla(s_r \rho_0 g_0)} - \overset{③}{\rho_0 \nabla\phi_1} + \hat{r} g_0 \overset{④}{\nabla\cdot(\rho_0 \underline{s})}$$

$$\nabla^2 \phi_1 = -4\pi G \, \nabla\cdot(\rho_0 \underline{s})$$

① Elastic

② Advection of stress

③ Change in grav. pot'l.

④ buoyancy

Look for solution

$$\underline{s} = \underline{s}_k e^{i\omega_k t}$$

Expand $\underline{s}_k$ in vector spherical harmonics

$$\underline{s}_k = \hat{r}\, U + \nabla_1 V - \hat{r} \times \nabla_1 W$$

$$\nabla_1 = \hat{\theta} \frac{\partial}{\partial\theta} + \hat{\phi}\, \mathrm{cosec}\,\theta \frac{\partial}{\partial\phi}$$

$$U = \sum_{\ell,m} U_\ell^m(r)\, Y_\ell^m(\theta,\phi)$$

⇒ separate variables

$$\Rightarrow \quad -\rho\omega_k^2 W = \frac{d}{dr}(\mu Z) + \frac{1}{r}\left[3\mu Z - \frac{\mu W}{r}(\ell+2)(\ell-1)\right]$$

$$Z = \frac{dW}{dr} - \frac{W}{r}$$

(Toroidal Modes)

+ 3 coupled 2nd order ODE's for spheroidal modes

Mode solution

1) Choose l

2) Choose ω_k

3) Integrate equation to surface

4) Does traction vanish ? (y_2)

No → 2)

Yes

pull out frequency & eigenfunction $(W(r))$

5) Compute elastic energy

$$\Rightarrow \int_V \underline{\epsilon}^* : \underline{\underline{C}} : \underline{\epsilon} \, dV$$

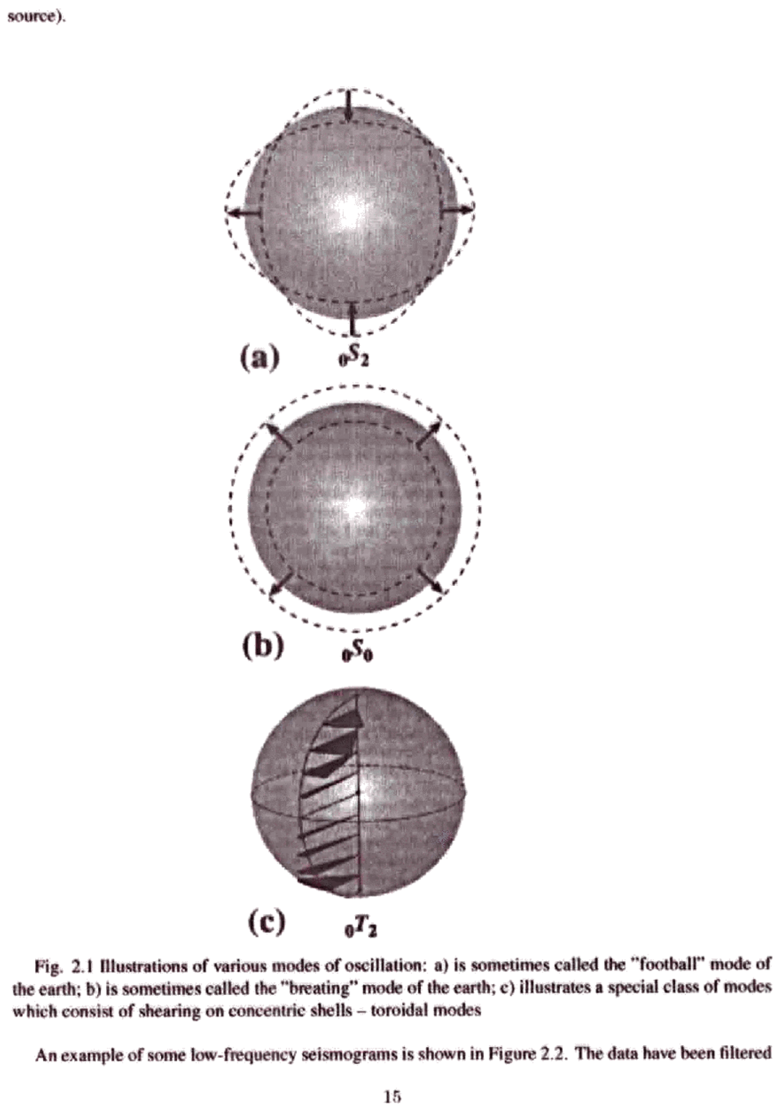

source).

Fig. 2.1 Illustrations of various modes of oscillation: a) is sometimes called the "football" mode of the earth; b) is sometimes called the "breating" mode of the earth; c) illustrates a special class of modes which consist of shearing on concentric shells – toroidal modes

An example of some low-frequency seismograms is shown in Figure 2.2. The data have been filtered

15

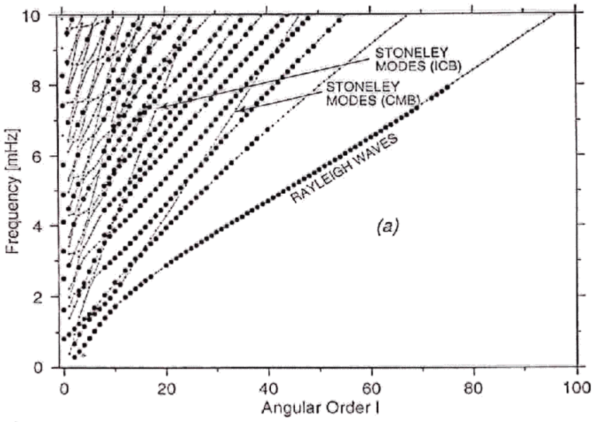
10
8
6
4
2
0
Frequency [mHz]
STONELEY MODES (ICB)
STONELEY MODES (CMB)
RAYLEIGH WAVES
(a)
0
20
40
60
80
100
Angular Order l

Fig 3·3

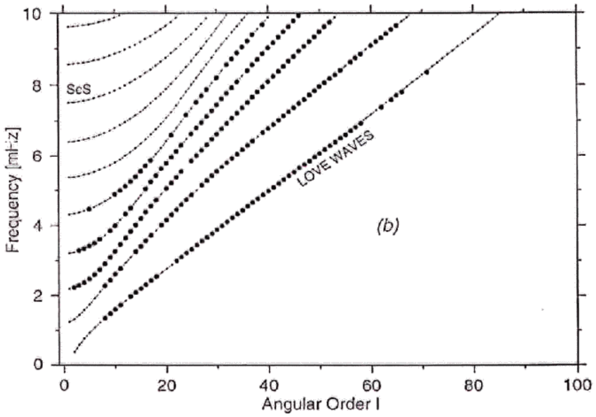
10
8
6
4
2
0
Frequency [mHz]
ScS
LOVE WAVES
(b)
0
20
40
60
80
100
Angular Order l

Fig 3·2

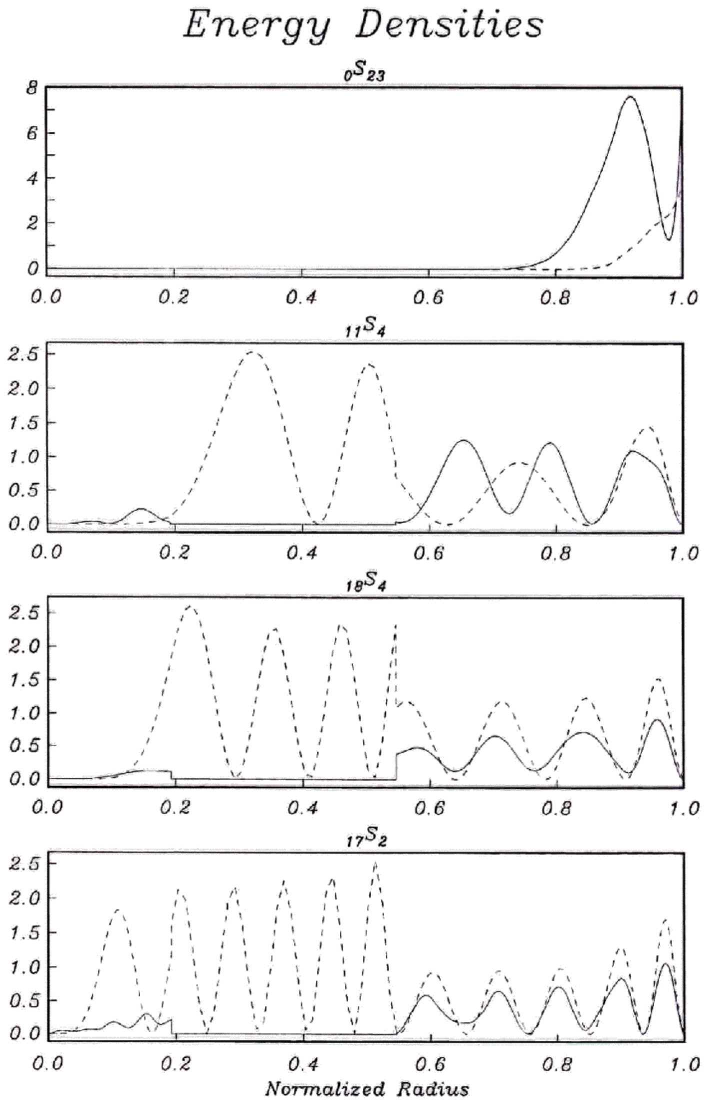
Energy Densities
$_0S_{23}$
8
6
4
2
0
0.0
0.2
0.4
0.6
0.8
1.0
$_{11}S_4$
2.5
2.0
1.5
1.0
0.5
0.0
$_{18}S_4$
$_{17}S_2$
Normalized Radius

Peak Shift plotted at great circle pole

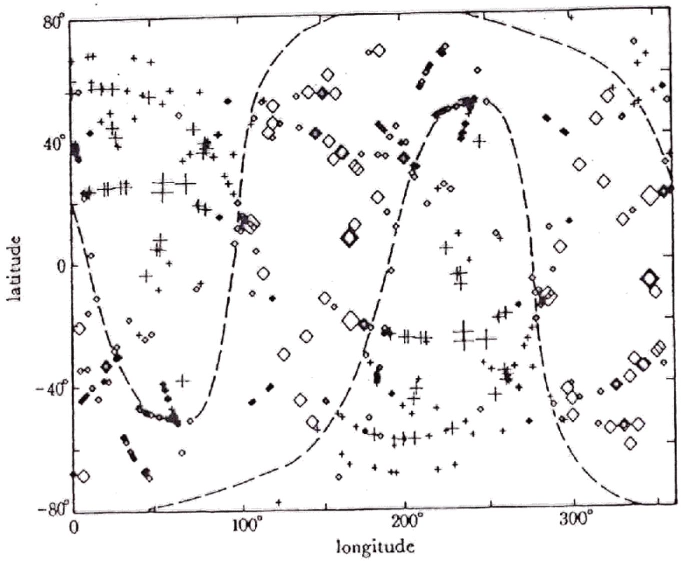

Figure 13. The effect of aspherical structure on center frequency can be seen by plotting the shift in frequency as a function of the pole position of the great circle joining source and receiver. Each symbol is plotted at a pole position: a + corresponds to a positive frequency shift and a corresponds to a negative frequency shift. The size of the symbol is indicative of the magnitude of the shift: the smallest symbols correspond to a 0–0.1% shift and the largest to a 0.3–0.4% shift. A degree-two spherical harmonic pattern accounts for most of the structure in the observations; the nodal lines of this pattern are shown by the dashed lines. This example is a combination of measurements for the modes ${}_0S_{21} - {}_0S_{23}$.

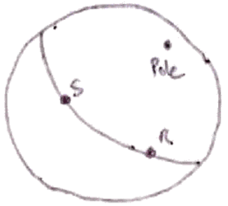

Consider j^{th} recording

$$u_j(t) = \sum_k A_{kj} \cos(\omega_k t + \phi_{kj}) e^{-\alpha_k t}$$

F.T. ⇒

$$u_j(\omega) = \sum_k A_{kj} \, C_k(\omega)$$

↑ spectrum of decaying cosinusoid

$$\Rightarrow \quad \underline{u}(\omega) = \underline{\underline{A}} \cdot \underline{c}(\omega)$$

$$\therefore \quad \underline{c}(\omega) = \underline{\underline{A}}^{-1} \cancel{\cdot}\, \underline{u}(\omega)$$

↑ do for multiplets or singlets

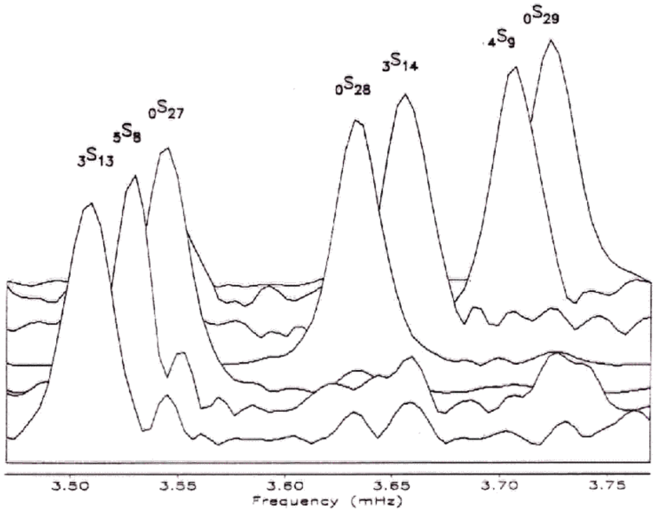

Figure 2.7 The results of multiplet stripping in a small frequency band which includes the fundamental spheroidal modes $_0S_{27}$ and $_0S_{28}$. The target multiplets are (front to back) $_3S_{13}$, $_5S_8$, $_0S_{27}$, $_0S_{28}$, $_3S_{14}$, $_4S_9$ and $_0S_{29}$. Note that overtones such as $_3S_{14}$ are clearly separated from the highly excited fundamental modes.

Both the fundamental toroidal and spheroidal modes are extremely well recovered with this technique. Figure 2.8 shows the resonance function for $_0S_l$ ($l = 8 \rightarrow 30$) plotted on a frequency axis relative to the predicted frequency of model PREM. Figure 2.9 is the corresponding plot for $_0T_l$ ($l = 8 \rightarrow 30$). These figures illustrate the biasing effects of mode-mode coupling. The distinctive kinks in the ω/l curves are due to Coriolis coupling between the two mode types and whole sequences of observations can be systematically shifted (*Masters et al. 1983*). Coriolis coupling is well understood and the apparent degenerate frequency can be reasonably accurately calculated except for very strongly coupled pairs. Most of our observations can therefore be corrected for Coriolis coupling effects. Strong coupling (*e.g.*, $_0S_{11} - {_0T_{12}}$, $_0S_{19} - {_0T_{20}}$) cannot be reliably predicted at present due to the sensitivity of the computation to the frequency spacing of the coupling multiplets and the lack of a separation into distinct lumps of energy. The dominant effect of coupling is a repelling of the coupling multiplets in real part frequency. Thus we can deduce from Figures 2.8 and 2.9 that the frequency of $_0S_{11}$ must be slightly greater than the

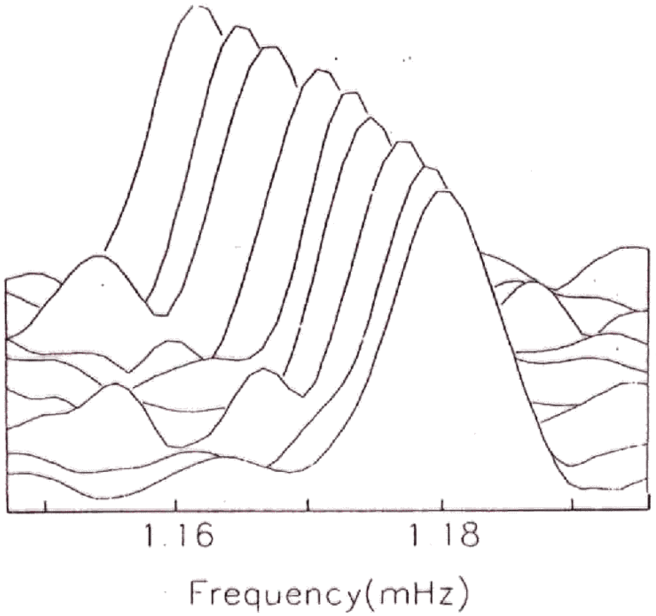

Figure 1.15. This figure has the same format as fig1.14 but now each row is the amplitude spectrum of a singlet of $_1S_4$. All nine singlets are recovered and follow a quadratic in azimuthal order close to that predicted for a rotating hydrostatic Earth.

1.3 References .

Chao, B.F., and F. Gilbert, Autoregressive estimation of complex eigenfrequencies in low frequency seismic spectra. *Geophys. J. R. Astron. Soc.*, **63**, 641–657, 1980.

Dahlen, F.A., The effect of data windows on the estimation of free oscillation parameters. *Geophys. J. R. Astron. Soc.*, **69**, 537–549, 1982.

Harris, F., On the use of windows for harmonic analysis with the discrete Fourier transform. *Proc. IEEE*, **66**, 51–83, 1978.

Masters, G., and F. Gilbert, Attenuation in the earth at low frequencies. *Phil. Trans. R. Soc. London*, **A308**, 479–522, 1983.

Thomson, D.J., Spectrum estimation and harmonic analysis. *IEEE Proc.*, **70**, 1055–1096, 1982.